



2

NRL Memorandum Report 6607

DTIC FILE COPY

Common-Mode Rejectors For Pulse Power Diagnostics

J. MATHEW

Beam Physics Branch
Plasma Physics Division

February 15, 1990

AD-A218 096

DTIC
ELECTE
FEB 16 1990
S B D
Co

Approved for public release; distribution unlimited.

90

02

57

REPORT DOCUMENTATION PAGE				Form Approved OMB No. 0704-0188	
1a. REPORT SECURITY CLASSIFICATION UNCLASSIFIED			1b. RESTRICTIVE MARKINGS		
2a. SECURITY CLASSIFICATION AUTHORITY		3. DISTRIBUTION / AVAILABILITY OF REPORT Approved for public release; distribution unlimited.			
2b. DECLASSIFICATION / DOWNGRADING SCHEDULE					
4. PERFORMING ORGANIZATION REPORT NUMBER(S)			5. MONITORING ORGANIZATION REPORT NUMBER(S)		
6a. NAME OF PERFORMING ORGANIZATION NRL Memorandum Report 6607	6b. OFFICE SYMBOL (if applicable) Code 4795	7a. NAME OF MONITORING ORGANIZATION			
6c. ADDRESS (City, State, and ZIP Code) Washington, DC 20375-5000			7b. ADDRESS (City, State, and ZIP Code)		
8a. NAME OF FUNDING / SPONSORING ORGANIZATION Office of Naval Research	8b. OFFICE SYMBOL (if applicable)	9. PROCUREMENT INSTRUMENT IDENTIFICATION NUMBER 47-1485-0-0			
8c. ADDRESS (City, State, and ZIP Code) Arlington, VA 22217-5000			10. SOURCE OF FUNDING NUMBERS		
		PROGRAM ELEMENT NO 61153N	PROJECT NO N0003987 WRZ00209-41	TASK NO RR011-09-41	WORK UNIT ACCESSION NO
11. TITLE (Include Security Classification) Common-Mode Rejectors for Pulse Power Diagnostics					
12. PERSONAL AUTHOR(S) Mathew, Joseph					
13a. TYPE OF REPORT Interim	13b. TIME COVERED FROM _____ TO _____	14. DATE OF REPORT (Year, Month, Day) 1990 February 15		15. PAGE COUNT 30	
16. SUPPLEMENTARY NOTATION					
17. COSATI CODES			18. SUBJECT TERMS (Continue on reverse if necessary and identify by block number)		
FIELD	GROUP	SUB-GROUP	Common-mode rejectors Diagnostics		
			Pulse power		
19. ABSTRACT (Continue on reverse if necessary and identify by block number)					
<p>Pulse power diagnostics are usually prone to common-mode noise pickup. A sure way of suppressing this noise is to introduce a common-mode rejector in each suspected signal line. Two types of rejectors have been developed. One handles signals with risetimes exceeding 10 ns, or equivalently with frequencies less than 35 MHz. The other is suitable even for signals with subnanosecond risetime. Both have been optimized to yield the highest rejection achievable. The method of winding employed and the interlead separation have been found to be quite important for proper operation of the common-mode rejector. Some of the underlying mechanisms of ground noise generation are also briefly investigated.</p>					
20. DISTRIBUTION / AVAILABILITY OF ABSTRACT <input checked="" type="checkbox"/> UNCLASSIFIED/UNLIMITED <input type="checkbox"/> SAME AS RPT <input type="checkbox"/> DTIC USERS			21. ABSTRACT SECURITY CLASSIFICATION UNCLASSIFIED		
22a. NAME OF RESPONSIBLE INDIVIDUAL Joseph Mathew			22b. TELEPHONE (Include Area Code) (202) 767-3135	22c. OFFICE SYMBOL Code 4795	

CONTENTS

INTRODUCTION	1
I. INDUCED VOLTAGES	1
II. GROUND CURRENT INTERACTIONS	3
III. REMEDIES	5
IV. HIGH FREQUENCY REJECTOR	6
V. ULTRA HIGH FREQUENCY REJECTOR	9
VI. CONCLUDING REMARKS	11
ACKNOWLEDGEMENTS	12
REFERENCES	12
DISTRIBUTION LIST	19

Accession For	
NTIS GRA&I	<input checked="" type="checkbox"/>
DTIC TAB	<input type="checkbox"/>
Unannounced	<input type="checkbox"/>
Justification	
By _____	
Distribution/	
Availability Codes	
Dist	Avail and/or Special
A-1	



COMMON-MODE REJECTORS FOR PULSE POWER DIAGNOSTICS

INTRODUCTION

Pulse power machines typically generate pulses with voltages ranging from 100 kV to 10 MV at currents in the 1 kA to 10 MA range. Pulse durations are usually less than 1 μ s. Ground noise can be severe in such environments. The large magnetic fields associated with these machines can induce voltages on the order of 50 kV in ground loops formed between signal cables and the machine ground return. For typical 100 foot long signal lines, ground loop inductances are on the order of 10 μ H. It is easy to see from $V = Ldi/dt$, that ground currents exceed 1 kA, 200 ns into the pulse.

It is instructive to review some of the underlying mechanisms of ground noise generation in pulse power environments, in order to fully appreciate the need for common-mode rejectors and their construction. Sporadic treatment of this subject may be found in much of the available literature. Many, however, discuss ground currents in the context of low power instrumentation techniques.¹

I. INDUCED VOLTAGES

Induced voltages in ground loops can be avoided if sufficient care is taken in the design of the pulse power machine and its associated diagnostics. Principles of electromagnetic topology² can be successfully applied to develop designs immune to noise. A complete

shield is needed around the machine. The diagnostic room should be a shielded enclosure and signal cable shields should be securely connected (no pigtails) at both ends to the respective shield rooms. If the conductivity of all shields is infinite, then the system should be immune to noise.

Very often, however, conditions are not as ideal. It is usually inconvenient to locate the machine in a shielded enclosure. Signal cables usually terminate on the outer shell of the machine, which also serves as the return current carrying conductor. Large windows in the shell distort the current flow pattern. Some magnetic flux leaks out, and voltages could be induced in local loops formed by adjacent cables. Return currents can be very large in the case of low impedance diodes, or arcs at the load. Resistive joints in the return path usually cause mild arcing, and substantial ground noise is introduced in the diagnostic cables.

Some pulse power components, for example Marx generators, striplines, etc. are housed in an oil tank, with signal cables terminating at specific points on the pulse power circuit, rather than at the tank wall. The cable shields are tied to the local circuit ground if the diagnostic device is a voltage divider, a capacitive probe, or a current shunt. The ground connection is sometimes improperly made using just a pigtail. The cable routing is also far from ideal in some cases. A substantial amount of ground noise is usually introduced in these arrangements. The inductance of the Marx or stripline current return conductor can elevate the potential of local grounds with respect to the diagnostic room ground. A single "contaminated" cable can cause ground currents to flow in other "healthy" ones. In this respect the various interactions with all the trigger circuits and cables should also be considered. There are also various stray capacitances between sensor

elements and high voltage surfaces, that can drive common-mode currents in some signal cables.

Switches employed in pulse power machines generate inordinately large amounts of rf noise. Cables with braided outer conductors invariably pickup both common-mode and difference-mode rf noise. Helix³ and Flexwell⁴ cables with solid corrugated copper outer conductors are relatively immune to such pickup. Radio frequency waves also travel along transmission lines formed by the signal cables and the nearby ground plane. A diagnostic shield room is necessary to prevent these waves from interacting with oscilloscopes or digitizers.

Finally, there are instances where a pulse power machine is used for beam generation in charged particle accelerators. Time varying magnetic fields are sometimes employed for inductive acceleration. Ground loops assume a great deal of importance in such instances.

II. GROUND CURRENT INTERACTIONS

Large ground currents, by themselves, need not necessarily introduce noise in measured signals. Common-mode currents flow exclusively in the outer shield. This is because of the additional self inductance faced by common-mode currents in the center conductor(s). An important means of interaction with the difference-mode signal occurs via the resistive voltage drop in the outer shield. The dc resistance of a 100-foot length of 1/2-inch Helix cable is 60 m Ω . For 1 kA ground current, the resistive drop is 60 V. For times much larger than the magnetic diffusion time of the outer shield (typically 10 μ s), this voltage drop directly adds to or subtracts from the difference-mode signal at the oscilloscope. The noise is much larger than typical signal levels in this specific example. Times of interest are

usually much less than the shield diffusion time. For these short time scales, the resistive drop is much larger due to skin effect. However, the voltage drop does not appear on the inside surface of the shield until times on the order of the diffusion time. Hence there is no noise introduced in the measured signals. Nonetheless, the voltage drops are large enough that even a small fraction diffusing in (over time scales of 100 ns) can cause noticeable errors in the signals. Braided cables are much more noisy in this respect. Any voltage appearing on the inside shield surface causes additional capacitive currents to flow to the inner conductor. A small fraction of the common-mode current also flows in the inner conductor due to finite conductivity effects. This causes a voltage to appear across the (50 Ω) terminating resistor. For times on the order of the cable transit time, the interaction is complicated due to transmission line effects, but the net result is a lower signal to noise ratio. Triaxial cables, configured properly, can eliminate these interactions. However, they do not provide complete immunity against other interactions described below. Additionally, low loss high frequency cables are usually available only as coaxial lines.

Another interaction occurs at the sensor due to its proximity to ground currents and high voltage surfaces. Ground currents can inductively couple to the sensor depending upon its geometric construction. Various electrostatic couplings can also introduce difference-mode noise. This is especially so when the cable shield is not "tied" to the machine, or when the connection is not sound. Once a common-mode to difference-mode conversion occurs at the sensor, it is virtually impossible to separate the noise from the signal.

Extremely good joints are called for at all cable connectors and splices. Loose connections cause nonuniform current flows that greatly increase crosstalk with the inner

conductor. BNC connectors are not as rugged as Type N connectors in this respect. Large ground currents can also cause mild arcing at resistive joints. This is especially important at diagnostic room penetrations where the arcs can radiate rf directly into the shielded enclosure.

III. REMEDIES

The most straightforward solution is to block the flow of ground currents, or at least maintain them at modest levels. Fiber optic analog links completely eliminate ground currents. They are, however, quite expensive for bandwidths exceeding 200 MHz, and require frequent maintenance. Isolating pulse transformers are another possibility. But it is virtually impossible to build one with adequate high frequency response and simultaneous high voltage isolation capability. The capacitance between primary and secondary windings provides a low impedance path for high frequency ground currents.

Another approach introduces a large common-mode inductor in the 110 V power line to the diagnostic shield room. However, this approach does not get rid of ground currents flowing in local loops formed by adjacent signal lines. Also, the diagnostic room could be elevated in potential with respect to ground, thus constituting an electrical safety hazard.

A sure way of controlling all ground currents is to employ a common-mode rejector with each suspected signal line. This is accomplished by winding the signal cable over a core of magnetic material. The rejector itself may be introduced at any convenient location between the pulse power machine and the diagnostic room. The machine ground is thereby isolated from the diagnostic room ground. The rejector may also be used to investigate the presence of ground noise in a particular signal line. Described below are two common-

mode rejectors that are somewhat optimized to give the highest rejection achievable. The first handles signals with risetimes exceeding 10 ns, or with frequencies less than 35 MHz. The second is an ultra high frequency rejector for signals with risetimes in excess of 0.5 ns.

IV. HIGH FREQUENCY REJECTOR

A reasonably large inductance common-mode rejector can be built for signal risetimes exceeding 10 ns. The rejector inductance should be much larger than typical ground loop inductances, in order to justify its introduction. A large number of turns may be used on a magnetic core if subminiature coaxial cable (say, RG-174/U) is used. One cannot, however, arbitrarily increase the number of turns to yield large values of inductance. Multilayer windings needed for this purpose have such large capacitances between layers that most of the rejector inductance is shorted out at the frequencies of interest. The problem is so severe that even the distance between the in-out leads becomes a determining factor. This effect is illustrated by the traces in Fig. 1.

A Tektronix Model FG-504 Function Generator was employed to generate a pulse with 10 ns risetime. Insulated wire with outer dimensions approximating those of RG-174/U, was used to build a ferrite cored inductor. Approximately 150 turns were wound in one layer. The inductor was connected in series with another loop of wire with roughly $20 \mu\text{H}$ inductance (to simulate the ground loop inductance of typical signal lines). The current through this combination due to the input pulse was monitored by measuring the voltage across a 50Ω series resistor. A 250 pF blocking capacitor was also introduced to prevent core saturation due to the -18V quiescent dc output of the generator.

Fig. 1a shows the function generator output measured before the blocking capacitor.

The pulse amplitude is seen to be ~ 35 V, and the risetime ~ 10 ns. The current waveform appears in Fig. 1b for the case where the in-out leads of the rejector barely touch one another. Large oscillations are seen, presumably due to ringing between the parasitic capacitance at the leads and the $20 \mu\text{H}$ loop inductance. One may estimate from the initial 12 mA current spike, a value for the parasitic capacitance of ~ 2 pF. This is a reasonable value, in view of the fact that the dielectric constant for most ferrites is ~ 10 for the frequencies of interest⁵. For the current trace in Fig. 1c, the winding was rearranged to increase the lead separation to 2 cm. The estimated interlead capacitance for this case is ~ 0.2 pF. The parasitic oscillations are greatly reduced, and the temporal behavior for longer times is consistent with the proper operation of the rejector.

Based on the results of this experiment, a common-mode rejector was built using RG-174/U. A simplified diagram of this rejector appears in Fig. 2. The minimum lead separation was maintained at 2 cm. Type M_2 Ni-Zn ferrite⁶ was used for the core. Two 1.6 cm thick discs with inner diameter 6.4 cm and outer diameter 14.8 cm were taped together to form the core. The resistivity of M_2 ferrite was $\sim 1 \times 10^7 \Omega\text{-cm}$ and the initial permeability was ~ 40 up to a frequency of ~ 50 MHz (Snoek limit⁷). The maximum number of turns that could be accommodated on the core was 97, giving an inductance of ~ 2 mH. The winding was single layered except on the very inside of the core. The interturn capacitance was therefore minimal. Over a 2 cm section midway between the two ends, the winding was three-layered on the inside, but still single-layered on the outside as shown in Fig. 2. The additional capacitance at this section would not increase the overall capacitance noticeably, because it would be in series with other much smaller turn to turn capacitances. Parasitic oscillations were observed to be negligibly small as in Fig. 1c.

A higher permeability ferrite (with a lower Snoek limit) could have been used. But a high frequency ferrite was chosen to yield a rejector impedance that was predominantly inductive throughout the frequency range of interest. The dielectric constant of ferrites usually increases considerably to values in the $10^3 - 10^4$ range as the frequency is lowered to ~ 1 kHz. Some ferrites with high permeability and low resistivity can have even higher dielectric constants⁵. Dimensional resonances assume importance in some of these cases because the dimensions are comparable to the wavelength of electromagnetic propagation in these media. Standing waves are set up, and rejector performance degrades appreciably.

The usefulness of a common-mode rejector depends to a large extent on the diagnostic environment. Fig. 3 shows current traces obtained with and without the rejector described above. The sensor was a Rogowski coil prone to common-mode pickup. The measured signal is the current in a 10 m long trigger cable shorted at the far end. Eight such cables were fed by a trigger generator delivering a maximum of 16 kA at 50 kV no load voltage. The common-mode rejector was introduced between two lengths of Flexwell coaxial cable, just a few feet from the generator. Considerable rf noise is expected at this location. Even so, the rejector functions admirably well. The lower trace is displaced ~ 100 ns in time due to the additional transit time in the 17 m cable used for the winding.

The frequency response of the rejector to difference-mode signals is determined by the length of cable used for the winding. The high frequency components of a signal are preferentially attenuated in a coaxial cable primarily due to the frequency dependent skin resistance of the inner and outer conductors. Fig. 4 shows the difference-mode response of the rejector. The function generator was used again to output a 250 ns wide pulse through a $0.1 \mu\text{F}$ blocking capacitor. A 50Ω Power Tee split the output pulse and transmitted two

half amplitude pulses in two 50Ω cables. One cable excited the common-mode rejector, while the other went directly to a dual beam oscilloscope. Both pulses were subsequently terminated in 50Ω and monitored on the scope.

The signal transmitted through the rejector is delayed approximately 100 ns as expected. The attenuation predicted for a 17 m length of RG-174 is ~ 3 db at 35 MHz (corresponding to the 10 ns risetime of the input signal). This is roughly consistent with the signal amplitudes in Fig. 4. Fast rising signals usually have limited pulse lengths. The 3 db attenuation figure is fully significant only for pulses with infinite duration. For short duration pulses, the distortion is not as severe. If the transmitted pulse in Fig. 4 is scaled in magnitude by ~ 1.3 , the resulting waveform would be quite similar to the generator output waveform. It is also a simple matter to generate a computer code to correct the data for the cable response, when the distortion is small as is the case here. Signals with risetimes exceeding 10 ns can therefore be successfully handled by the rejector.

V. ULTRA HIGH FREQUENCY REJECTOR

The requirements are a lot more stringent for an ultra high frequency rejector. The cable response desired for ultra fast signals can only be achieved with a much shorter length of RG-174. The capacitance shunting the rejector also needs to be greatly reduced. Both requirements can be readily achieved by stringing a large number of ferrite beads on a short length of cable. The surge impedance of the beads is what limits the common-mode current at all frequencies above the Snoek limit.

Consider, for example, a rejector for risetimes exceeding 0.5 ns, or equivalently, for frequencies less than 700 MHz. Approximately 100 ferrite beads are strung on a meter

length of RG-174. The bead dimensions are : 0.32 cm inner diameter, 0.64 cm outer diameter, and 0.95 cm long. A frequent choice for the bead material is Type H Ni-Zn ferrite⁶, or equivalent. Typical catalog values for Type H ferrite are : initial permeability ~ 850 , volume resistivity $\sim 1 \times 10^5 \Omega\text{-cm}$, saturation flux density $\sim 3.4 \text{ kG}$, and Snoek limit $\sim 3 \text{ MHz}$.

Ferrite shield beads are usually used at frequencies much greater than the Snoek limiting frequency, above which initial permeability decreases rapidly, and losses increase proportionately. This behavior is usually attributed to the onset of ferromagnetic resonance in the anisotropy field⁵. The empirical formula $\mu_i f_r \approx 3 \times 10^9 \text{ Hz}$ for Ni-Zn ferrites⁷, is also explained by this phenomenon. μ_i is the initial permeability, and f_r is the limiting frequency. Higher permeability ferrites have lower bandwidths according to this relation.

The insertion impedance of a ferrite bead is predominantly inductive below the Snoek limiting frequency, but becomes resistive for all frequencies greatly exceeding the limit. For common-mode rejection it hardly matters whether the impedance is inductive or resistive as long as the current is limited. Catalog numbers for the 3 MHz bead referenced above suggest an insertion impedance of $\sim 40 \Omega$ at 25 MHz, 66Ω at 100 MHz, 57Ω at 700 MHz, and 51Ω at 1 GHz. The impedance does not increase linearly with frequency as would be the case if the bead acted as an inductor. The total impedance for 100 beads is $5.7 \text{ k}\Omega$ at 700 MHz. For a 50 kV ground induced voltage, the common-mode current is therefore limited to a value less than 0.9 A. This represents a considerable reduction from the kiloampere levels expected without the rejector, 100 ns into the pulse.

The inductance of a single bead below the Snoek limit is $\sim 1.2 \mu\text{H}$. The rejector inductance is therefore $120 \mu\text{H}$, which is much greater than typical ground loop inductances.

It is, however, at least an order of magnitude smaller than typical values attained for the high frequency rejector. Fortunately, large rejector inductances are normally not required because pulse durations are usually small for machines requiring ultra fast diagnostics. In the rare event that very high frequency common-mode noise is superimposed over low frequency (kilohertz type) noise due to slow rising external magnetic fields, for example, the signal can be capacitively coupled to "break the low frequency ground loop". Capacitors need to be employed both in the signal line and in the ground (return) line. This is best done at the sensor. If they are introduced at a different location along the signal transmission path, they should be carefully constructed to minimize rf interference. Another option is to employ sensors immune to low frequency common-mode noise.

The attenuation for difference-mode signals for a meter of RG-174 is 0.8 db at 700 MHz. As a result, for limited duration pulses, distortion levels are expected to be a few percent. The common-mode rejector described has discrimination capabilities close to the maximum achievable for ultra fast signals. Knowing the criteria for efficient common-mode rejection, it is conceivable that a somewhat more optimized rejector can be built.

VI. CONCLUDING REMARKS

Pulse power diagnostics are frequently vulnerable to common-mode pickup. Signals can be reliably measured in such environments if a common-mode rejector is employed with each suspected signal line. Two different types of rejectors have been described. The high frequency rejector is suitable for signals with risetimes exceeding 10 ns, or equivalently for frequencies less than 35 MHz. The ultra high frequency rejector can be used for signals with subnanosecond risetime. Both employ ferrite cores for fast response.

Control of common-mode currents addresses only part of the problem of noise pickup. The other aspect deals with spurious difference-mode pickup at the sensor, which is outside the scope of this paper. The classic example is the difference between a shielded and an unshielded Rogowski coil when it is employed near high voltages. The large capacitive currents flowing to the unshielded coil can easily induce spurious signals due to a variety of higher order effects. A careful analysis of any diagnostic arrangement can usually indicate the underlying mechanism of noise generation. J. C. Martin, one of the early pioneers of pulse power technology, noted⁸ "... there is no 'black magic' in pickup : the laws of electromagnetism apply here just as anywhere else." In general, noise problems can be averted if reasonable care is taken in the design of the sensor. Even better performance is achieved if diagnostics are incorporated early on in the design phase of the machine.

ACKNOWLEDGEMENTS

This work was supported by the U. S. Office of Naval Research. C. A. Kapetanacos and J. Golden of the Modified Betatron Section deserve special thanks for their support and encouragement.

REFERENCES

1. R. Morrison, *Grounding and Shielding Techniques in Instrumentation* (Wiley, New York, 1967).
2. W. Graf, "Practical Shielding and Grounding Techniques", *Fast Electrical and Optical Measurements*, 1 (Martinus Nijhoff Publishers, Boston, 1986).
3. Andrew Corporation, Orland Park, Illinois.
4. Cablewave Systems, North Haven, Connecticut.

5. J. Smit and H. P. J. Wijn, *Ferrites* (Wiley, New York, 1959).
6. National Magnetics Group Inc., Newark, New Jersey.
7. J. K. Watson, *Applications of Magnetism* (Wiley, New York, 1980).
8. J. C. Martin, "Nanosecond Pulse Techniques", *Pulsed Electrical Power Circuit and Electromagnetic System Design Notes*, Air Force Weapons Laboratory Report AFWL-TR-73-166 (1973).

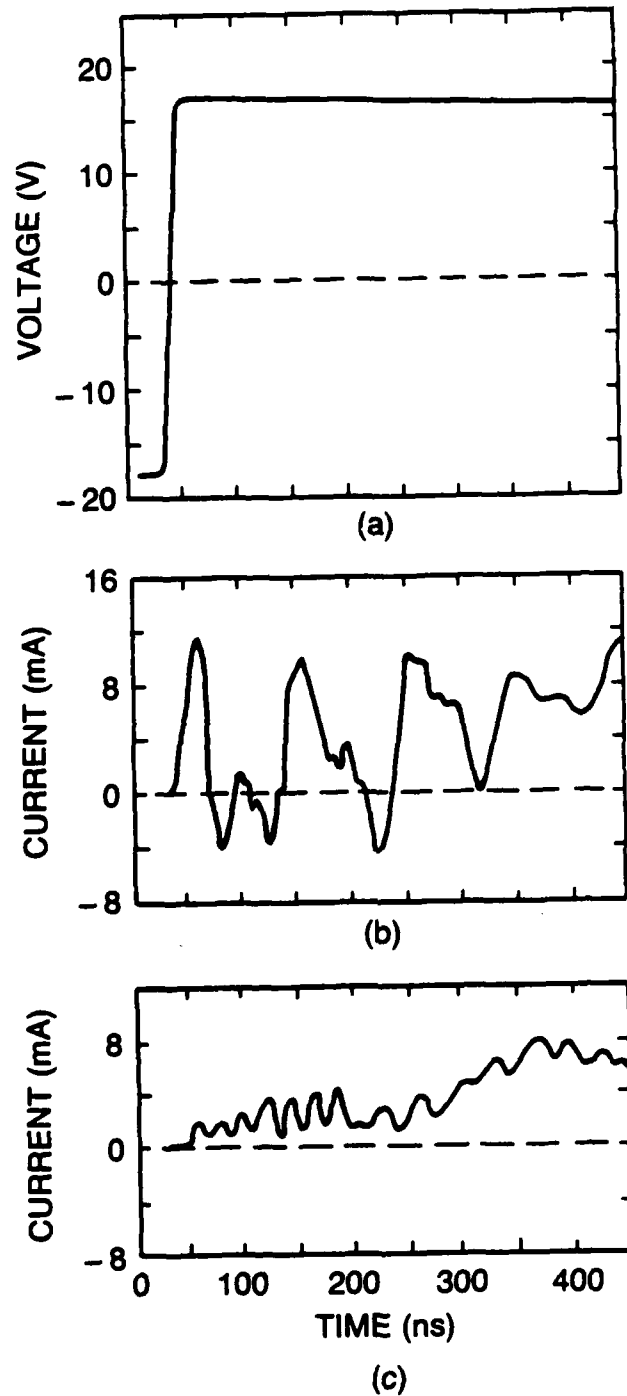


FIG. 1. (a) Function generator output measured before the blocking capacitor.

(b) Common-mode current for the case where the leads barely touch one another.

Scope sensitivity: 0.2 V/div.

(c) Common-mode current for 2 cm lead separation.

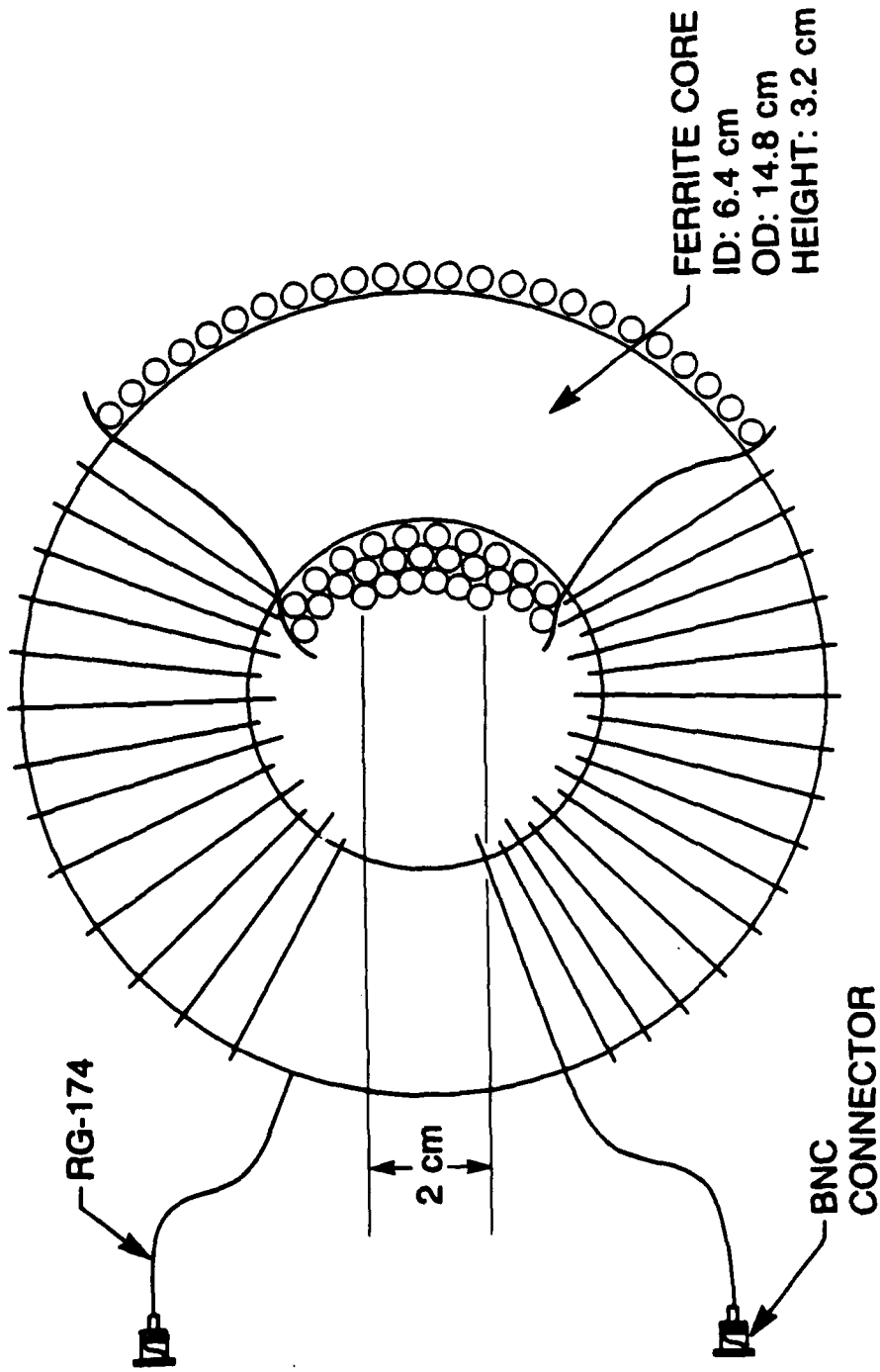


FIG. 2. Simplified diagram of the high frequency common-mode rejector. The number of

turns is 97; much fewer turns are shown for clarity.

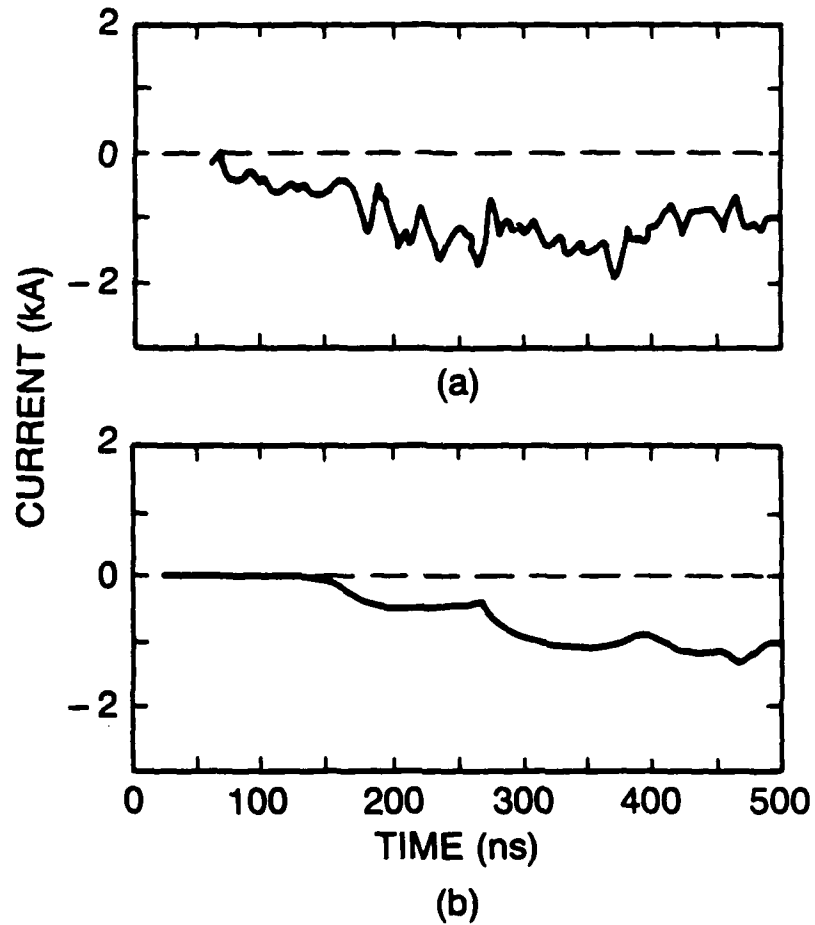


FIG. 3. (a) Signal trace obtained without the rejector. Scope sensitivity: 1 V/div.

(b) Signal measured with the rejector for the same experimental setup as in (a).

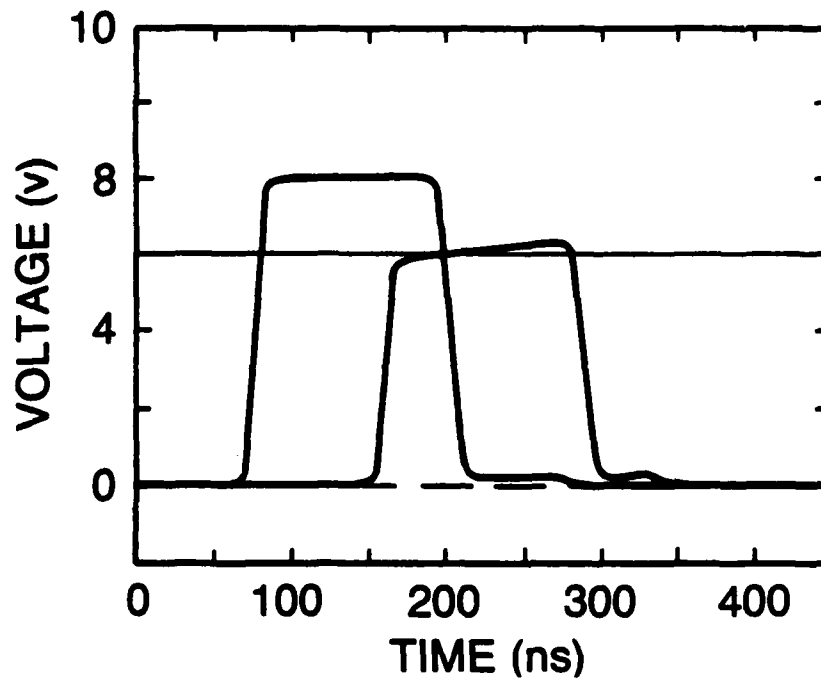


FIG. 4. Difference-mode response of the common-mode rejector showing the input pulse from the signal generator, and the delayed pulse transmitted through the rejector. The 6 V reference line is a guide for the eye.

DISTRIBUTION LIST
(Revised December 18, 1989)

Dr. M. Allen
Stanford Linear Accelerator Center
Stanford, CA 94305

Dr. W. Barletta
Lawrence Livermore National Laboratory
P.O. Box 808
Livermore, CA 94550

Dr. M. Barton
Brookhaven National Laboratory
Upton, L.I., NY 11101

Dr. Jim Benford
Physics International Co.
2700 Merced St.
San Leandro, CA 94577

Dr. Kenneth Bergerson
Plasma Theory Division - 5241
Sandia National Laboratories
Albuquerque, NM 87115

Dr. Daniel Birx
Lawrence Livermore National Laboratory
P.O. Box 808
Livermore, CA 94550

Dr. Charles Brau
Vanderbilt University
Nashville, TN 37235

Dr. R. Briggs
SSC Laboratory
2550 Beckleymeade Ave.
Suite 260
Dallas, TX 75237

Dr. Allan Bromborsky
Harry Diamond Laboratory
2800 Powder Mill Road
Adelphi, MD 20783

Dr. H. Lee Buchanan
DARPA
1400 Wilson Blvd.
Arlington, VA 22209-2308

Dr. M. Butram
Sandia National Laboratory
Albuquerque, NM 87115

Dr. M. Caponi
TRW Advance Tech. Lab.
I Space Park
Redondo Beach, CA 90278

Prof. F. Chen
Department of Electrical Engineering
University of California at Los Angeles
Los Angeles, CA 90024

Dr. D. Chernin
Science Applications Intl. Corp.
1710 Goodridge Drive
McLean, VA 22102

Prof. R. Davidson
Plasma Fusion Center
M.I.T.
Cambridge, MA 02139

Dr. J. Dawson
University of California at Los Angeles
Department of Physics
Los Angeles, CA 90024

Dr. W.N. Destler
Department of Electrical Engineering
University of Maryland
College Park, MD 20742

Dr. H. Dreicer
Director Plasma Physics Division
Los Alamos Scientific Laboratory
Los Alamos, NM 87544

Prof. W.E. Drummond
Austin Research Associates
1901 Rutland Drive
Austin, TX 78758

Dr. Don Eccleshall
Bldg. 120-Room 241
Ballistic Research Lab.
Aberdeen Proving Grounds
Aberdeen, MD 21005

Dr. J.G. Eden
Department of Electrical Engineering
University of Illinois
155 EEB
Urbana, IL 61801

Dr. A. Faltens
Lawrence Berkeley Laboratory
Berkeley, CA 94720

Dr. T. Fessenden
Lawrence Livermore National Laboratory
P.O. Box 808
Livermore, CA 94550

Dr. A. Fisher
Physics Department
University of California
Irvine, CA 92664

Prof. H.H. Fleischmann
Laboratory for Plasma Studies and
School of Applied and Eng. Physics
Cornell University
Ithaca, NY 14850

Dr. T. Fowler
Associate Director
Magnetic Fusion Energy
Lawrence Livermore National Laboratory
P.O. Box 808
Livermore, CA 94550

Mr. George B. Frazier, Manager
Pulsed Power Research & Engineering Dept.
2700 Merced St.
P.O. Box 1538
San Leandro, CA 94577

LCDR W. Fritchie
Space and Naval Warfare
Systems Command
Attention: Code PMW145B
Washington, DC 20363-5100

Dr. S. Graybill
Harry Diamond Laboratory
2800 Powder Mill Road
Adelphi, MD 20783

Lt. Col. R. Gullickson
SDIO-DEO
Pentagon
Washington, DC 20301-7100

Dr. Z.G.T. Guiragossian
TRW Systems and Energy RI/1070
Advanced Technology Lab
1 Space Park
Redondo Beach, CA 90278

Prof. D. Hammer
Laboratory of Plasma Physics
Cornell University
Ithaca, NY 14850

Dr. David Hasti
Sandia National Laboratory
Albuquerque, NM 87115

Dr. C.E. Hollandsworth
Ballistic Research Laboratory
DRDAB - BLB
Aberdeen Proving Ground, MD 21005

Dr. C.M. Huddleston
ORI
1375 Piccard Drive
Rockville, MD 20850

Dr. S. Humphries
University of New Mexico
Albuquerque, NM 87131

Dr. Robert Hunter
9555 Distribution Ave.
Western Research Inc.
San Diego, CA 92121

Dr. J. Hyman
Hughes Research Laboratory
3011 Malibu Canyon Road
Malibu, CA 90265

Prof. H. Ishizuka
Department of Physics
University of California at Irvine
Irvine, CA 92664

Dr. D. Keefe
Lawrence Berkeley Laboratory
Building 50, Rm. 149
One Cyclotron Road
Berkeley, CA 94720

Dr. Donald Kerst
University of Wisconsin
Madison, WI 53706

Dr. Edward Knapp
Los Alamos Scientific Laboratory
Los Alamos, NM 87544

Dr. A. Kolb
Maxwell Laboratories
8835 Balboa Ave.
San Diego, CA 92123

Dr. Peter Korn
Maxwell Laboratories
8835 Balboa Ave.
San Diego, CA 92123

Dr. R. Linford
Los Alamos Scientific Laboratory
P.O. Box 1663
Los Alamos, NM 87545

Dr. C.S. Liu
Department of Physics
University of Maryland
College Park, MD

Prof. R.V. Lovelace
School of Applied and Eng. Physics
Cornell University
Ithaca, NY 14853

Dr. S.C. Luckhardt
Plasma Fusion Center
M.I.T.
Cambridge, MA 02139

Dr. J.E. Maenchen
Division 1241
Sandia National Lab.
Albuquerque, NM 87511

Prof. T. Marshall
School of Engineering and Applied Science
Plasma Laboratory
S.W. Mudd Bldg.
Columbia University
New York, NY 10027

Dr. M. Mazarakis
Sandia National Laboratory
Albuquerque, NM 87115

Dr. D.A. McArthur
Sandia National Laboratories
Albuquerque, NM 87115

Prof. J.E. McCune
Dept. of Aero. and Astronomy
M.I.T.
77 Massachusetts Ave.
Cambridge, MA 02139

Prof. G.H. Miley, Chairman
Nuclear Engineering Program
214 Nuclear Engineering Lab.
Urbana, IL 61801

Dr. Bruce Miller
TITAN Systems
9191 Town Centre Dr.
Suite 500
San Diego, CA 92122

Dr. A. Mondelli
Science Applications International Corp.
1710 Goodridge Drive
McLean, VA 22102

Dr. Phillip Morton
Stanford Linear Accelerator Center
Stanford, CA 94305

Dr. M. Nahemow
Westinghouse Electric Corporation
1310 Beutah Rd.
Pittsburg, PA 15235

Prof. J. Nation
Lab. of Plasma Studies
Cornell University
Ithaca, NY 14850

Dr. V.K. Neil
Lawrence Livermore National Laboratory
P.O. Box 808
Livermore, CA 94550

Dr. Gene Nolting
Naval Surface Warfare Center
White Oak Laboratory
10901 New Hampshire Ave.
Silver Spring, MD 20903-5000

Dr. C.L. Olson
Sandia Laboratory
Albuquerque, NM 87115

Dr. Arthur Paul
Lawrence Livermore National Laboratory
P.O. Box 808
Livermore, CA 94550

Dr. S. Penner
National Institute of Standards
and Technology
Washington, D.C. 20234

Dr. Jack M. Peterson
Lawrence Berkeley Laboratory
Berkeley, CA 94720

Dr. R. Post
Lawrence Livermore National Lab.
P.O. Box 808
Livermore, CA 94550

Dr. Kenneth Prestwich
Sandia National Laboratory
Albuquerque, NM 87115

Dr. S. Prono
Lawrence Livermore National Lab.
P.O. Box 808
Livermore, CA 94550

Dr. Sid Putnam
Pulse Science, Inc.
600 McCormick Street
San Leandro, CA 94577

Dr. Louis L. Reginato
Lawrence Livermore National Lab
P.O. Box 808
Livermore, CA 94550

Prof. N. Reiser
Dept. of Physics and Astronomy
University of Maryland
College Park, MD 20742

Dr. M.E. Rensink
Lawrence Livermore National Lab
P.O. Box 808
Livermore, CA 94550

Dr. D. Rej
Lab for Plasma Physics
Cornell University
Ithaca, NY 14853

Dr. J.A. Rome
Oak Ridge National Lab
Oak Ridge, TN 37850

Prof. Norman Rostoker
Dept. of Physics
University of California
Irvine, CA 92664

Prof. George Schmidt
Physics Department
Stevens Institute of Tech.
Hoboken, NJ 07030

Philip E. Serafim
Northeastern University
Boston, MA 02115

Dr. Andrew Sessler
Lawrence Berkeley National Lab
Berkeley, CA 94720

Dr. John Siambis
Lockheed
Palo Alto Research Lab
3257 Hanover Street
Palo Alto, CA 94304

Dr. Adrian C. Smith
Ballena Systems Corp.
1150 Ballena Blvd.
Suite 210
Alameda, CA 94501

Lloyd Smith
Lawrence Berkeley National Laboratory
Berkeley, CA 94720

Dr. A. Sternlieb
Lawrence Berkely National Laboratory
Berkeley, CA 94720

Dr. D. Straw
W.J. Schafer Assoc.
2000 Randolph Road, S.E., Suite A
Albuquerque, NM 87106

Prof. C. Striffler
Dept. of Electrical Engineering
University of Maryland
College Park, MD 20742

Prof. R. Sudan
Laboratory of Plasma Studies
Cornell University
Ithaca, NY 14850

Dr. W. Tucker
Sandia National Laboratory
Albuquerque, NM 87115

Dr. H. Uhm
Naval Surface Warfare Center
White Oak Laboratory
10901 New Hampshire Ave. Code R41
Silver Spring, MD 20903-5000

Dr. William Weldon
University of Texas
Austin, TX 78758

Dr. Mark Wilson
NIST
Gaithersburg, MD 20899

Dr. P. Wilson
Stanford Linear Accelerator Center
Stanford, CA 94305

Prof. C.B. Wharton
303 N. Sunset Drive
Ithaca, NY 14850

Dr. Gerald Yonas
TITAN Systems
9191 Town Centre Drive
Suite 500
San Diego, CA 92122

*West Defense Technical Information Center - 2 copies

NRL Code 2628 - 20 copies

NRL Code 4700 - 26 copies

NRL Code 4790 - 3 copies

NRL Code 4795 - 40 copies

*Cameron Station
Alexandria, VA 22314
DDA-2 = 2

Director of Research
U.S. Naval Academy
Annapolis, MD 21402
(2 copies) Director

Naval Research Laboratory
Washington, DC 20375-5000
Code 2634
Timothy Calderwood Tim

MAILING LIST/FOREIGN

Library
Institut fur Plasmaforschung
Universitat Stuttgart
Pfaffenwaldring 31
7000 Stuttgart 80, West Germany

Ken Takayama
KEN, TRISTAN Division
Oho, Tsukuba, Ibaraki, 305 JAPAN